Supporting Information

Benzotriazole Loading in Confined ZIF-8@mSiO$_2$ Nanospaces for Waterborne Anticorrosion Coatings

Kwang Keat Leong[a], Minjun Kim[a]*, Asep Sugih Nugraha[a], Jeffrey Venezuela[b], Yusuf Valentino Kaneti[a], Muxina Konarova[c], Yusuke Yamauchi[a,d]*, Yuan Ma[e], Nasim Amiralian[a]*

[a] Australian Institute for Bioengineering and Nanotechnology (AIBN), The University of Queensland, Brisbane, Queensland 4071, Australia

[b] School of Mechanical and Mining Engineering, Faculty of Engineering, Architecture and Information Technology, The University of Queensland, Brisbane, Queensland 4071, Australia

[c] School of Chemical Engineering, The University of Queensland, Brisbane, Queensland 4071, Australia

[d] Department of Materials Process Engineering, Graduate School of Engineering, Nagoya University, Nagoya 464-8603, Japan

[e] Baoshan Iron & Steel Co., Ltd., Shanghai 201900, China

E-mails: n.amiralian@uq.edu.au (N.A.); y.yamauchi@uq.edu.au (Y.Y); minjun.kim@uq.edu.au (M.K.)

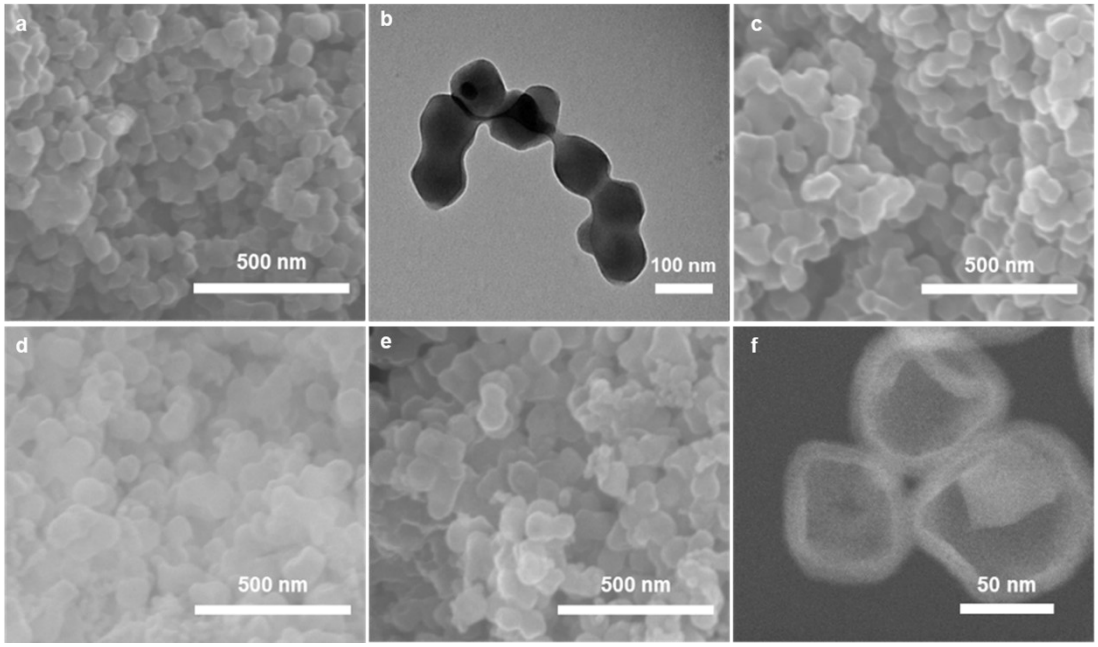

Figure S1. SEM image of (a) ZIF-8, TEM image (b) of BTA-ZIF-8. SEM image of (c) BTA-ZIF-8, (d) ZIF-8@$mSiO_2$, and (e) BTA-ZIF-8@$mSiO_2$. (f) HAADF-STEM image of the etched BTA-ZIF-8@$mSiO_2$.

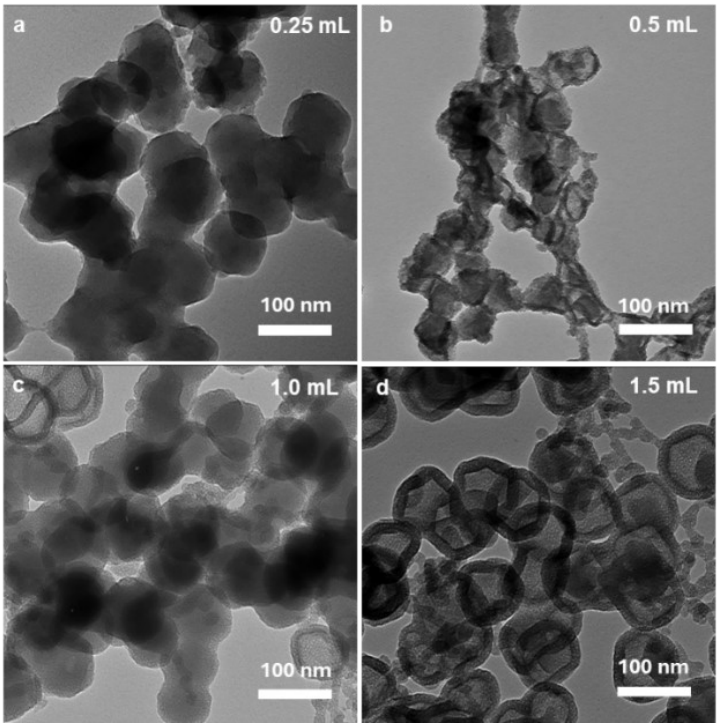

Figure S2. TEM images of ZIF-8@mSiO_2 synthesized using (a) 0.25 mL, (b) 0.5 mL, (c) 1.0 mL, and (d) 1.5 mL of 68.6 mM CTAB solution.

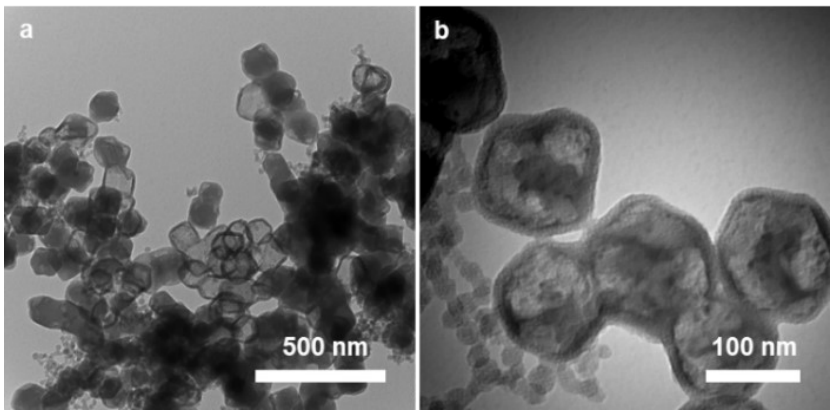

Figure S3. (a) Low-magnification and (b) high-magnification TEM images of the product obtained from coating ZIF-8 with $mSiO_2$ under water-based conditions.

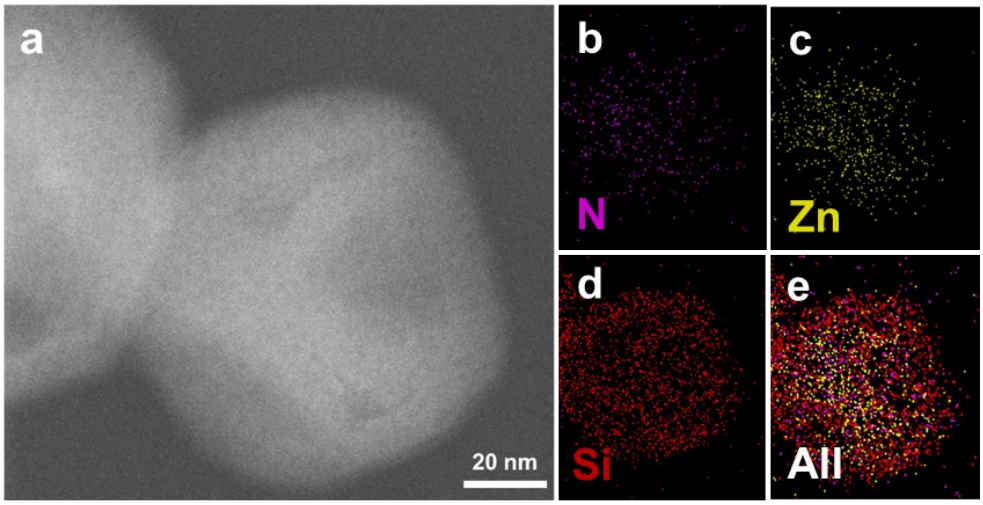

Figure S4. (a) HRTEM image of BTA-ZIF-8@mSiO_2 and respective elemental mappings for (b) N, (c) Zn, (d) Si, and (e) all.

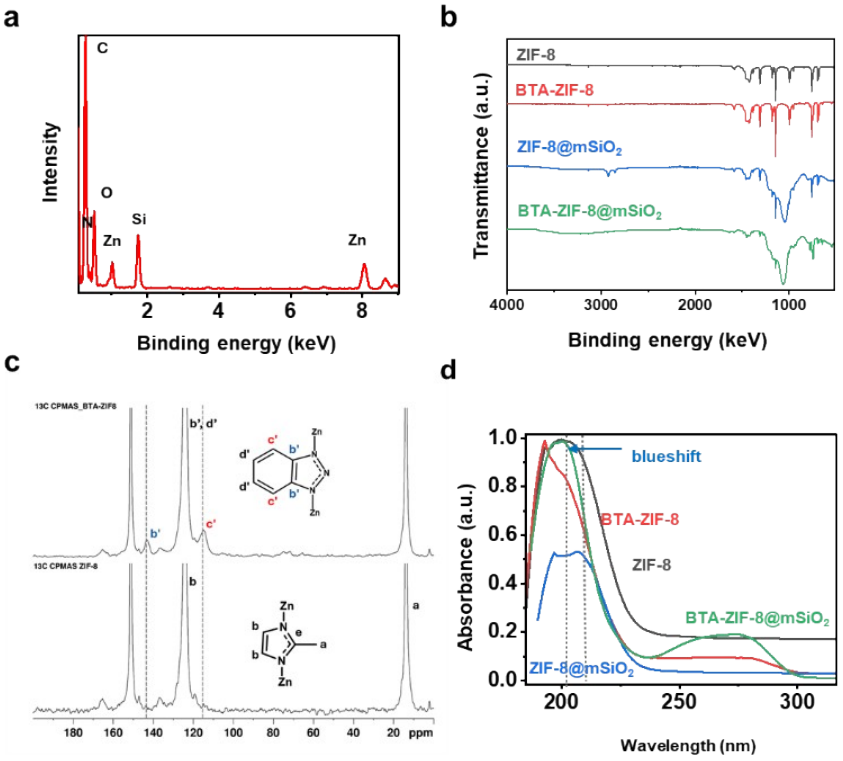

Figure S5. (a) EDS spectra obtained from HR-TEM mapping of BTA-ZIF-8@mSiO$_2$, confirming the presence of all constituent elements. (b) FTIR spectra of all nanoparticles. (c) ^{13}C CP-MAS NMR of BTA-ZIF-8 (top) and ZIF-8 (bottom). (d) UV-Vis spectra for the nanoparticles in water showing a blue shift after loading with BTA.

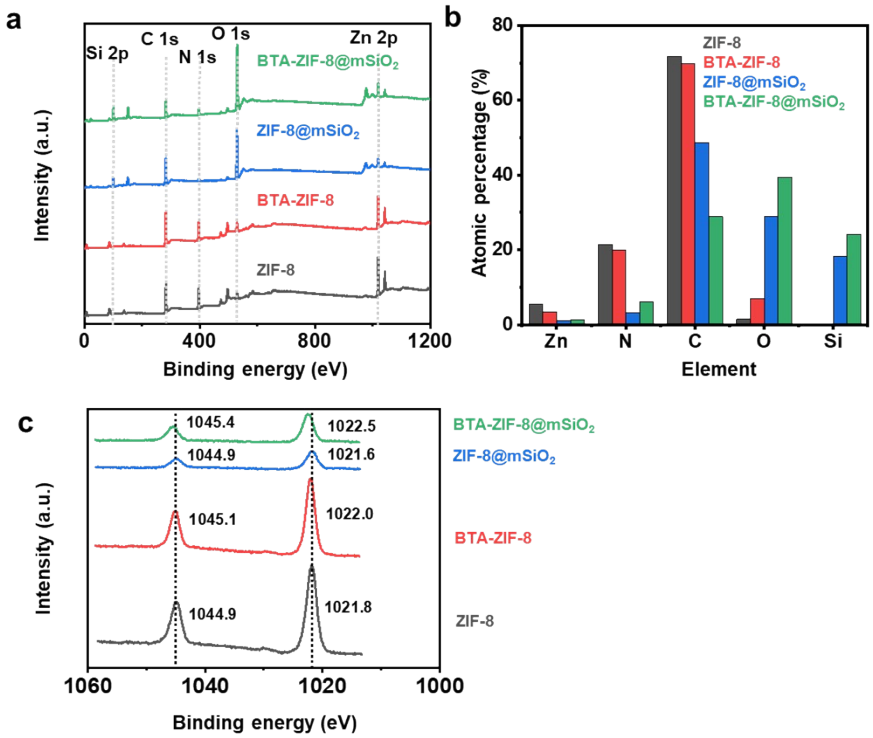

Figure S6. (a) Survey XPS spectra of ZIF-8, BTA-ZIF-8, ZIF-8@mSiO$_2$ and BTA-ZIF-8@mSiO$_2$. (b) Bar graph of atomic% of Zn, N, C, O and Si. (c) High-resolution XPS spectra for Zn 2*p*.

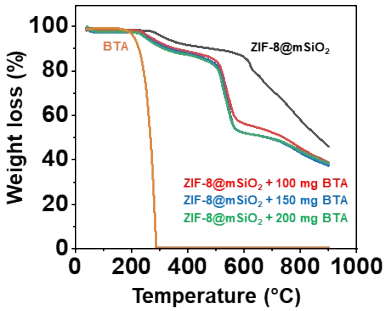

Figure S7. TGA curves of BTA-ZIF-8@mSiO$_2$ prepared with different initial loading amounts of BTA.

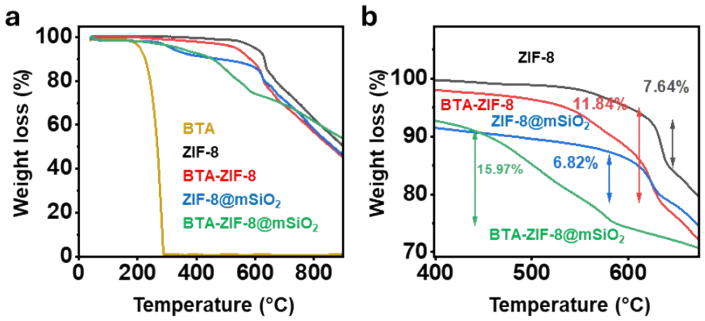

Figure S8. (a) TGA curves of BTA, ZIF-8, and various ZIF-8-based nanoparticles. (b) Enlarged view of the corresponding temperature range.

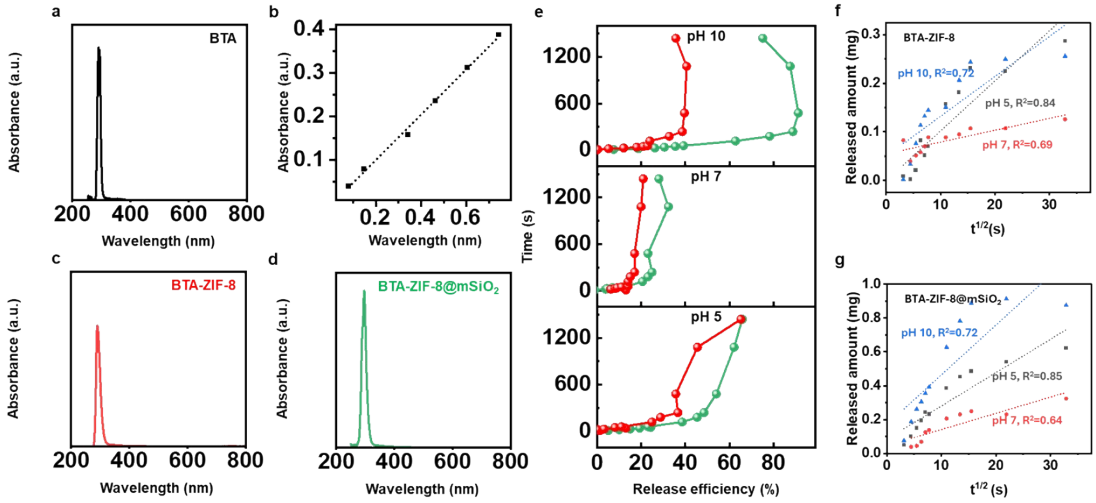

Figure S9. (a) UV-Vis absorbance of BTA. (b) Calibration curve used to quantify the released amount of BTA. Absorbance of (c) BTA-ZIF-8 and (d) BTA-ZIF-8@mSiO$_2$. (e) Time-dependent release efficiency at different pH values for BTA-ZIF-8 and BTA-ZIF-8@mSiO$_2$. Fitting of the release curve using Higuchi model for (f) BTA-ZIF-8 and (g) BTA-ZIF-8@mSiO$_2$.

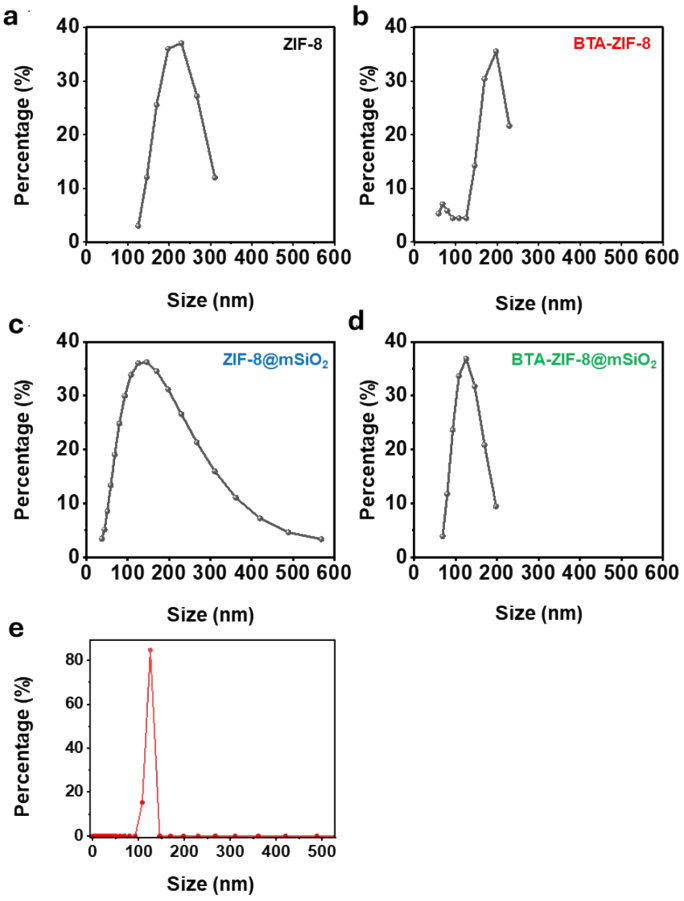

Figure S10. DLS particle size analysis for (a) ZIF-8, (b) BTA-ZIF-8, (c) ZIF-8@$mSiO_2$, and (d) BTA-ZIF-8@$mSiO_2$. (e) DLS particle size distribution of BTA-ZIF-8@$mSiO_2$ after 6 months of water immersion.

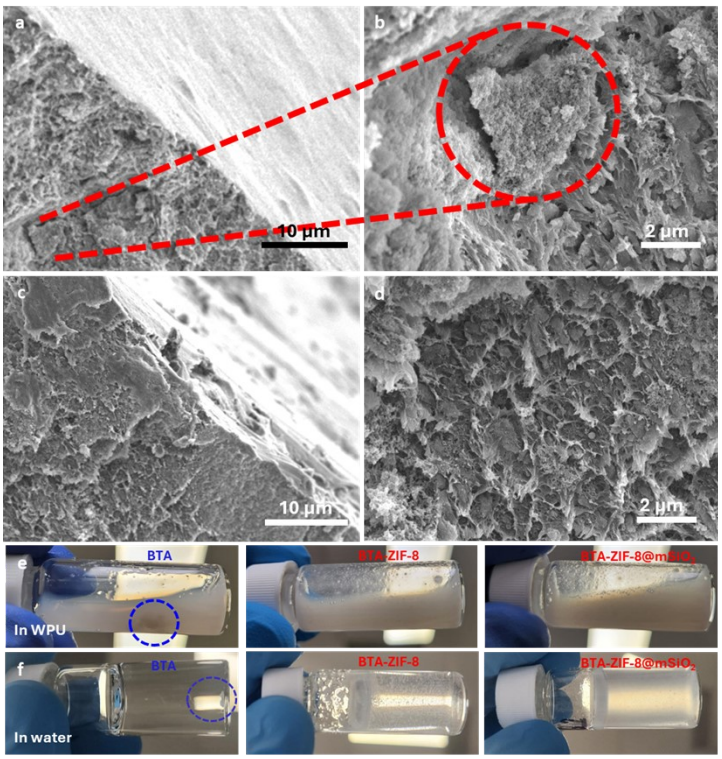

Figure S11. Cross-sectional SEM images for BTA-ZIF-8/WPU (a-b) and BTA-ZIF-8@$mSiO_2$/WPU (c-d) films. Dispersion tests of BTA, BTA-ZIF-8 and BTA-ZIF-8@$mSiO_2$ in waterborne polyurethane (e) and water (f).

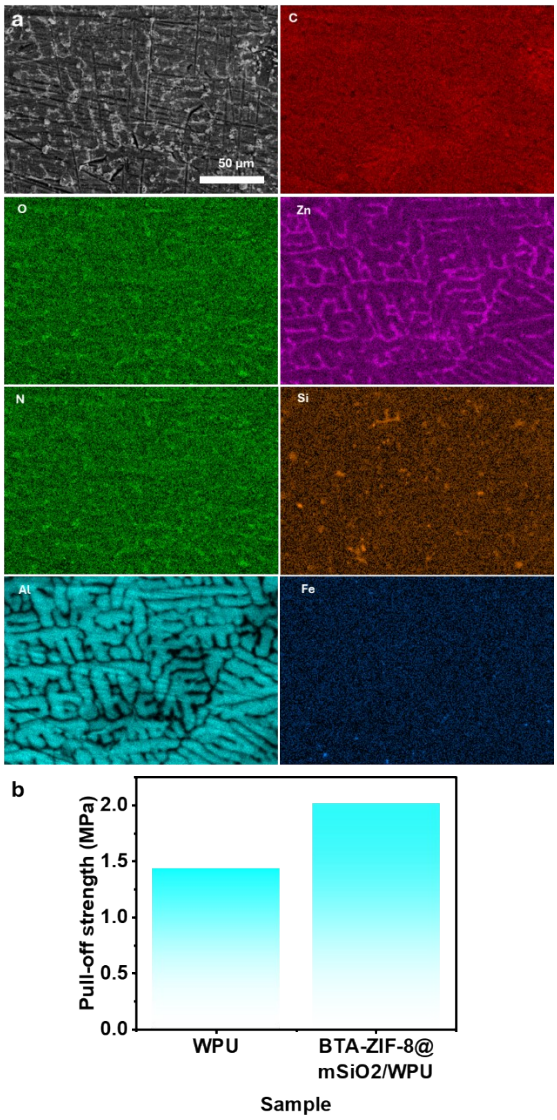

Figure S12. (a) EDS mapping images of BTA-ZIF-8@mSiO$_2$/WPU coating on Zn-plated steel. (b) Pull-off adhesion strength for WPU and BTA-ZIF-8@mSiO$_2$/WPU.

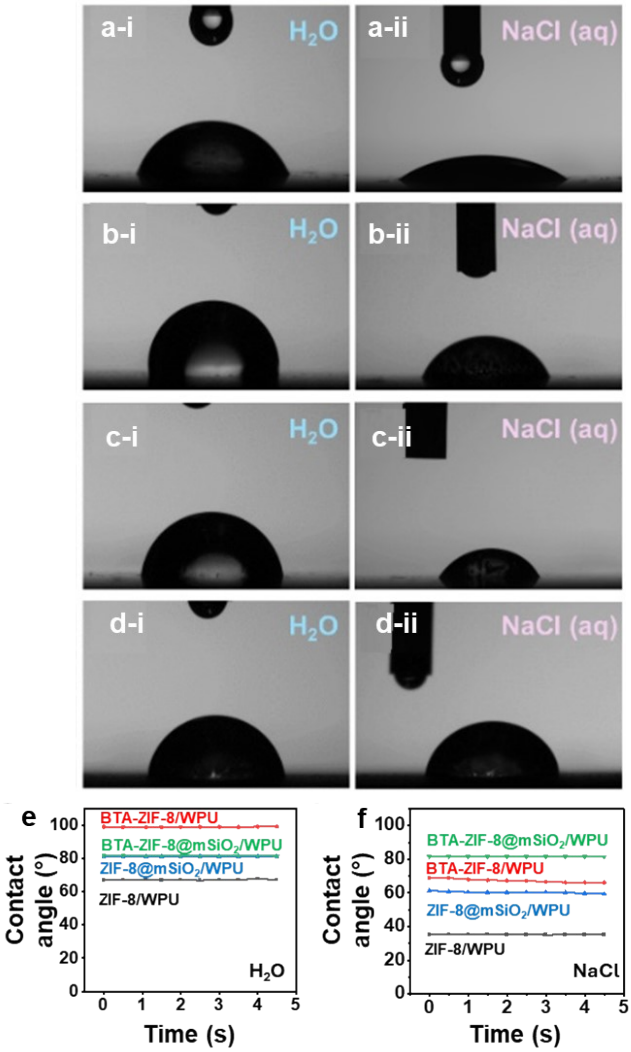

Figure S13. Contact angle images and corresponding measured values of the WPU film loaded with 3 wt.% of (a) ZIF-8, (b) BTA-ZIF-8, (c) ZIF-8@mSiO$_2$, and (d) BTA-ZIF-8@mSiO$_2$, tested with (i) water and (ii) 3.5 wt.% NaCl solution. The summarized contact angle values are shown in (e) for water and (f) for NaCl solution.

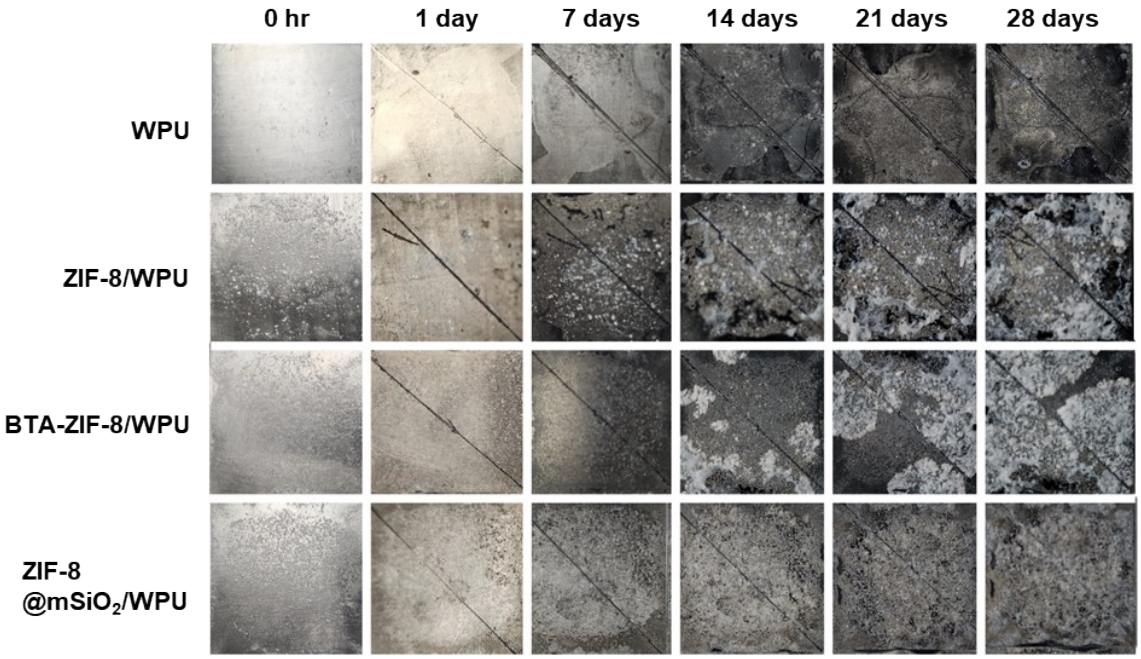

Figure S14. Images of steel plates coated with different coating compositions during the immersion test in 3.5 wt.% NaCl solution.

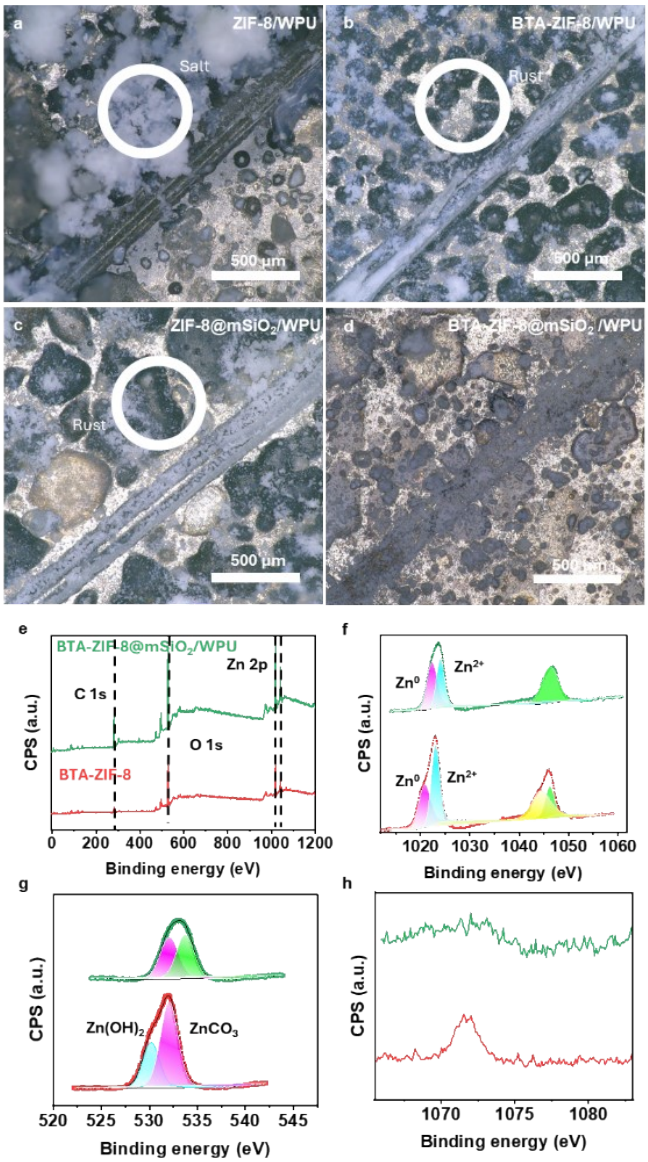

Figure S15. Optical microscopy images of post-immersion WPU coatings on steel plates containing 3 wt.% of (a) ZIF-8, (b) BTA-ZIF-8, (c) ZIF-8@$mSiO_2$, and (d) BTA-ZIF-8@$mSiO_2$. (e) The survey XPS spectra for BTA-ZIF-8@$mSiO_2$/WPU (green) and BTA-ZIF-8/WPU (red). High-resolution XPS for Zn 2*p* (f), O 1*s* (g), and Na 1*s* (h) for BTA-ZIF-8@$mSiO_2$/WPU (green) and BTA-ZIF-8/WPU (red).

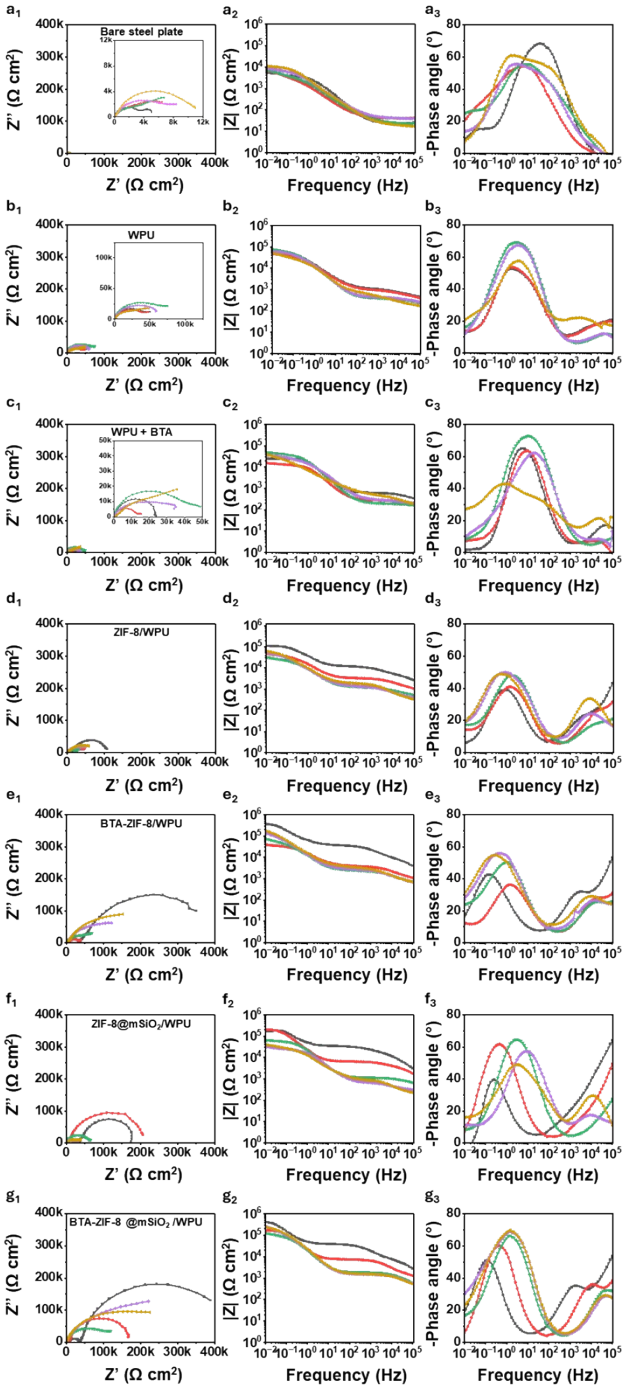

Figure S16. Impedance study of different coatings using 1) Nyquist plots, (2) Bode plots, and (3) phase angle plots for (a) bare steel plate, (b) WPU, (c) WPU + BTA, (d) ZIF-8/WPU, (e) BTA-ZIF-8/WPU, (f) ZIF-8@$mSiO_2$/WPU, and (g) BTA-ZIF-8@$mSiO_2$/WPU for day 0 (black), day 1 (red), week 1 (green), week 2 (purple) and week 3 (light yellow).

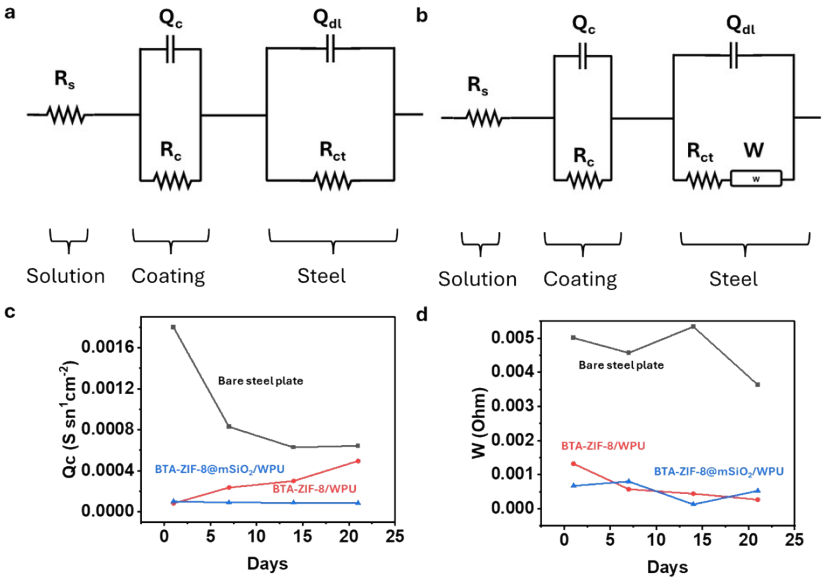

Figure S17. Equivalent circuit models used for fitting: (a) coating at day 0 and (b) coating from day 1 onwards. Equivalent circuit parameter evolution over time for coating capacitance (Q_c) (c) and Warburg element (W) (d).

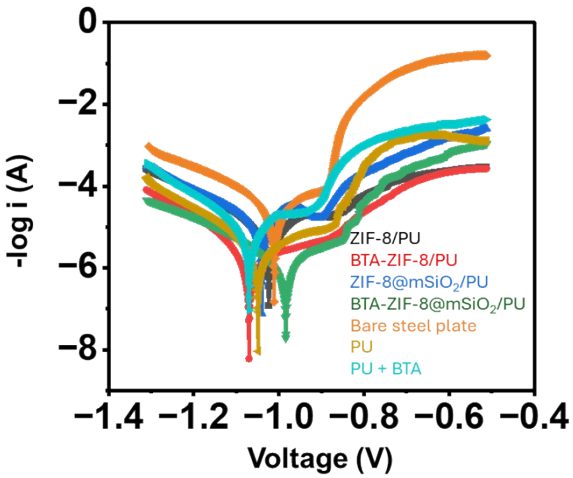

Figure S18. Potentiodynamic polarization measurements of the coatings with different compositions.

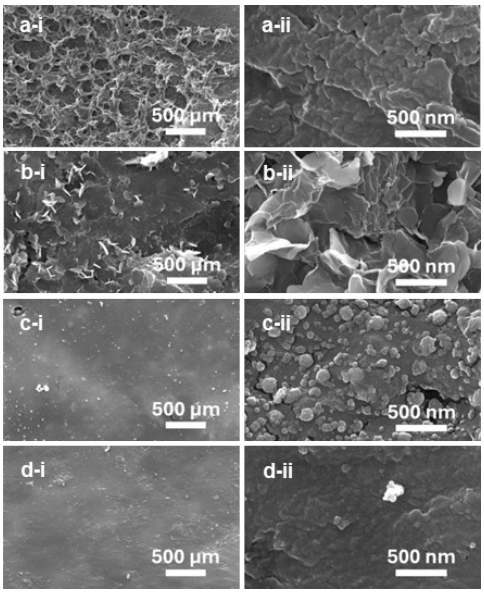

Figure S19. (i) Low- and (ii) high-magnification SEM images showing film morphology after EIS and potentiodynamic polarization tests for (a) ZIF-8/WPU, (b) BTA-ZIF-8/WPU, (c) ZIF-8@mSiO_2/WPU, and (d) BTA-ZIF-8@mSiO_2/WPU.

Table S1. Elemental distribution obtained from HR-TEM mapping of BTA-ZIF-8@mSiO$_2$.

Element	Percentage (%)
C	76.7
O	10.55
Si	7.52
Zn	3.92
N	0.76
Cl	0.28
Ca	0.26

Table S2. XPS elemental analyses of ZIF-8@$mSiO_2$ (top) and BTA-ZIF-8@$mSiO_2$ (bottom).

Name	Position	At%
O 1s	532.24	28.93
C 1s	284.83	48.68
N 1s	399.10	3.09
Zn 2p	1021.78	1.01
Si 2p	102.92	18.29

Name	Position	At%
O 1s	533.10	39.43
C 1s	285.10	28.90
N 1s	400.24	6.17
Zn 2p	1022.52	1.30
Si 2p	103.73	24.20

Table S3. Zeta potential values for different ZIF-8-derived nanoparticles.

Sample	ZIF-8	ZIF-8@$mSiO_2$	BTA-ZIF-8@$mSiO_2$
Values (mV)	17.85	-23.61	-21.01
	17.9	-22.65	-26.78
	18.94	-22.1	-23.1
Mean value (mV)	18.23	-22.79	-22.02
Standard deviation (mV)	0.6	0.8	3.0

Table S4. Average thickness of WPU thin films incorporating 3 wt.% nanoparticles on steel plates, determined using an Elcometer.

Sample	Thickness (µm)
ZIF-8/WPU	13.46
BTA-ZIF-8/WPU	20.36
ZIF-8@mSiO_2/WPU	22.00
BTA-ZIF-8@mSiO_2/WPU	17.83

Table S5. Roughness parameters obtained from DSX1000 light optical microscopy images for different coatings.

Sample	R_a (µm)	R_q (µm)
ZIF-8/WPU	0.290	0.379
BTA-ZIF-8/WPU	0.259	0.357
ZIF-8@$mSiO_2$/WPU	0.063	0.083
BTA-ZIF-8@$mSiO_2$/WPU	0.087	0.114

Table S6. Equivalent circuit parameters used for coating data fitting.

Film	Days	R_s ($\Omega \cdot cm^2$)	R_c ($\Omega \cdot cm^2$)	Q_c ($S\ s^{n1}\ cm^{-2}$)	R_{ct} ($\Omega \cdot cm^2$)	Q_{dl} ($S\ s^{n2}\ cm^{-2}$)	W
Bare steel plate	0	3.064	4.29×10^{2}	3.02×10^{-4}	5.46×10^{1}	1.74×10^{-4}	
	1	5.142	1.71×10^{2}	1.80×10^{-3}	9.90×10^{-1}	1.06×10^{-4}	5.01×10^{-3}
	7	3.053	1.99×10^{2}	8.30×10^{-4}	1.83×10^{0}	3.75×10^{-5}	4.57×10^{-3}
	14	5.331	4.79×10^{2}	6.28×10^{-4}	1.43×10^{1}	8.20×10^{-5}	5.34×10^{-3}
	21	2.282	6.75×10^{2}	6.43×10^{-4}	1.01×10^{-1}	2.35×10^{-5}	3.63×10^{-3}
WPU	0	61.1	4.58×10^{3}	6.66×10^{-5}	8.47×10^{1}	3.45×10^{-7}	
	1	49.73	2.74×10^{3}	1.02×10^{-4}	5.62×10^{1}	1.92×10^{-7}	8.26×10^{-4}
	7	27.05	6.04×10^{3}	1.19×10^{-4}	1.42×10^{1}	2.18×10^{-7}	1.35×10^{-3}
	14	31.09	4.99×10^{3}	1.08×10^{-4}	1.83×10^{1}	2.92×10^{-7}	1.78×10^{-3}
	21	22.51	1.89×10^{3}	1.76×10^{-4}	2.83×10^{1}	7.40×10^{-7}	7.65×10^{-4}
WPU + BTA	0	41.17	3.73×10^{1}	1.93×10^{-7}	2.83×10^{3}	4.92×10^{-5}	
	1	26.76	1.31×10^{3}	8.85×10^{-5}	8.72×10^{0}	1.51×10^{-5}	4.71×10^{-3}
	7	13.46	4.15×10^{3}	5.96×10^{-5}	8.56×10^{0}	8.12×10^{-8}	1.95×10^{-3}
	14	24.41	1.98×10^{3}	5.11×10^{-5}	7.12×10^{0}	4.73×10^{-7}	1.12×10^{-3}
	21	24.24	4.22×10^{2}	4.71×10^{-3}	3.16×10^{1}	3.38×10^{-7}	6.74×10^{-4}
ZIF-8/WPU	0	346.9	1.03×10^{3}	3.41×10^{-8}	1.04×10^{4}	4.21×10^{-5}	
	1	123.5	2.52×10^{3}	1.01×10^{-4}	2.50×10^{2}	5.48×10^{-8}	9.55×10^{-4}
	7	64.66	1.61×10^{3}	1.85×10^{-4}	7.64×10^{1}	1.57×10^{-7}	1.31×10^{-3}
	14	51.37	2.26×10^{3}	3.27×10^{-4}	8.84×10^{1}	2.42×10^{-7}	7.81×10^{-4}
	21	44.67	2.54×10^{3}	3.76×10^{-4}	1.47×10^{2}	2.41×10^{-7}	5.59×10^{-4}
BTA-ZIF-8/WPU	0	557.2	3.56×10^{3}	2.58×10^{-8}	3.50×10^{4}	5.48×10^{-5}	
	1	133.8	2.26×10^{3}	8.25×10^{-5}	3.27×10^{2}	6.10×10^{-8}	1.32×10^{-3}
	7	86.55	2.91×10^{3}	2.36×10^{-4}	1.67×10^{2}	8.99×10^{-8}	5.70×10^{-4}
	14	85.14	7.23×10^{3}	3.00×10^{-4}	1.80×10^{2}	1.05×10^{-7}	4.40×10^{-4}
	21	75.29	7.30×10^{3}	4.96×10^{-4}	2.22×10^{2}	9.61×10^{-8}	2.66×10^{-4}
ZIF-8@$mSiO_2$/WPU	0	285.7	1.54×10^{4}	5.62×10^{-5}	3.14×10^{3}	9.92×10^{-9}	1.11×10^{-3}
	1	147.5	1.83×10^{4}	1.00×10^{-4}	5.43×10^{2}	1.58×10^{-8}	4.44×10^{-4}
	7	57.05	5.64×10^{3}	5.95×10^{-5}	7.61×10^{1}	4.49×10^{-8}	1.17×10^{-3}
	14	39.52	2.13×10^{3}	4.68×10^{-5}	4.07×10^{1}	4.95×10^{-7}	1.59×10^{-3}
	21	30.09	1.75×10^{3}	9.73×10^{-5}	7.24×10^{1}	3.45×10^{-7}	8.86×10^{-4}
BTA-ZIF-8@$mSiO_2$/WPU	0	413.9	4.40×10^{4}	8.10×10^{-5}	3.80×10^{3}	4.21×10^{-8}	
	1	112.3	1.50×10^{4}	1.01×10^{-4}	6.64×10^{2}	4.11×10^{-8}	6.72×10^{-4}
	7	58.51	9.60×10^{4}	8.93×10^{-5}	1.44×10^{2}	5.15×10^{-8}	7.98×10^{-4}
	14	62.32	2.00×10^{4}	8.86×10^{-5}	1.28×10^{2}	7.14×10^{-8}	1.24×10^{-4}
	21	53.56	1.93×10^{4}	8.39×10^{-5}	1.10×10^{2}	6.57×10^{-8}	5.25×10^{-4}

Table S7. Electrochemical parameters obtained from potentiodynamic polarization measurements of the coatings after 3 weeks of immersion testing.

Sample	E_{corr} (V)	i_{corr} (A cm^{-2})	β_c (mV dec^{-1})	β_a (mV dec^{-1})
Bare steel plate	-1.10	4.19×10^{-5}	165.84	61.4
WPU	-1.05	3.67×10^{-6}	141.84	103.2
WPU + BTA	-1.07	1.41×10^{-5}	135.50	118.6
ZIF-8/WPU	-1.02	6.70×10^{-6}	149.25	256.1
BTA-ZIF-8/WPU	-1.07	1.51×10^{-6}	130.55	185.3
ZIF-8@mSiO_2/WPU	-1.04	8.26×10^{-6}	131.58	212.0
BTA-ZIF-8@mSiO_2/WPU	-0.98	9.90×10^{-7}	145.56	113.9